Journal of Magnetism and Magnetic Materials 459 (2018) 282–284

Contents lists available at ScienceDirect

Journal of Magnetism and Magnetic Materials

journal homepage: www.elsevier.com/locate/jmmm

Research articles

Proximity induced superconductivity in indium gallium arsenide quantum wells

K. Delfanazari [a,b,*], R.K. Puddy [b], P. Ma [b], T. Yi [b], M. Cao [b], Y. Gul [c], I. Farrer [b,d], D.A. Ritchie [b], H.J. Joyce [a], M.J. Kelly [a,b], C.G. Smith [b]

[a] Centre for Advanced Photonics and Electronics (CAPE), Electrical Engineering Division, University of Cambridge, Cambridge CB3 0FA, UK
[b] Department of Physics, Cavendish Laboratory, University of Cambridge, Cambridge CB3 0HE, UK
[c] Department of Electronic and Electrical Engineering, University College London, London WC1E 7JE, UK
[d] Department of Electronic and Electrical Engineering, University of Sheffield, Mappin Street, Sheffield S1 3JD, UK

ARTICLE INFO

Article history:
Received 10 July 2017
Received in revised form 10 October 2017
Accepted 14 October 2017
Available online 16 October 2017

ABSTRACT

We report on the experimental observation of the proximity induced superconductivity in an indium gallium arsenide ($In_{0.75}Ga_{0.25}As$) quantum well. The Josephson junction was fabricated by several photolithographic processes on an InGaAs heterojunction and Niobium (Nb) was used as superconducting electrodes. Owing to the Andreev reflections and Andreev bound states at the Nb-$In_{0.75}Ga_{0.25}As$ quantum well-Nb interfaces, the subharmonic energy gap structures (SGS) are observed at the differential conductance (dI/dV) versus voltage (V) plots when the applied source-drain bias voltages satisfy the expression $V_{SD} = 2\Delta/ne$. The dI/dV as a function of applied magnetic field B shows a maximum at zero B which decreases by increasing B. When decreasing B to below ±0.4 T, a hysteresis and shift of the conductance maxima close to $B = 0$ T are observed. Our results help to pave the way to the development of integrated coherent quantum circuitry.

1. Introduction

The proximity effect in hybrid superconductor-semiconductor (S-Sm) structures, e.g. superconducting correlations and supercurrent transport in a semiconductor connected to a superconductor mediated by phase coherent Andreev reflections [1–3], provides the possibility to study some fascinating fundamental physics such as Kondo-enhanced Andreev tunnelling [4], supercurrent reversal in quantum dots [5], Josephson quantum electron pumps [6]. There has been renewed interests in such systems after the observation of Majorana fermions states at the S-Sm interfaces [7–9]. This is because Majorana Zero modes have potential to support topologically protected quantum computing [10]. Yet, the fundamental technological problem is to fabricate a highly transparent contact between a superconductor with a high Fermi energy E_f and a semiconducting material with a low E_f.

In this regard, here we present our experimental results on proximity induced superconductivity in a high-mobility two-dimensional electron gas (2DEG) in an indium gallium arsenide ($In_{0.75}Ga_{0.25}As$) heterostructure. The symmetric and planar Nb-2DEG-Nb Josephson junction was fabricated on an InGaAs chip in which each junction consists of two identical Nb superconducting electrodes. The junction was measured by using a lock-in measurement technique in a dilution fridge with a base temperature of 40 mK.

Andreev reflections and bound states due to the electron and hole like quasiparticle correlations at the Nb-$In_{0.75}Ga_{0.25}As$ quantum well interfaces lead to the observation of a U-shape dip at low-bias voltage of the differential resistance dV/dI (V_{SD}) plot, as well as the subharmonic energy gap structures (SGS) at $V = 2\Delta/ne$ where the Δ is Nb superconducting gap. Both the induced gap and SGS features suppress significantly as temperature T and magnetic field B are applied to the system – due to the T and B dependences of Δ_{Nb} – leading to a shift of the SGS toward zero bias [11]. Sweeping dI/dV vs. B, results in the observation of a hysteresis for $-0.25 \leq B\ (T) \leq 0.25$ and a shift in the differential conductance maximum close to $B = 0$ T.

2. Materials and methods

The $In_{0.75}GaAs/In_{0.75}AlAs/GaAs$ quantum well were grown by molecular beam epitaxy (MBE) [11,12]. Eight identical and symmetric Josephson junctions (results for one junction is discussed here) were patterned and fabricated on a single chip. The 30 nm thick 2DEG with density $n_s = 2.24 \times 10^{11}$ (cm^{-2}) and mobility

* Corresponding author at: Electrical Engineering Division, University of Cambridge, Cambridge CB3 0FA, UK.
E-mail address: kd398@cam.ac.uk (K. Delfanazari).

https://doi.org/10.1016/j.jmmm.2017.10.057
0304-8853/

μ_e=2.5 × 10^5 (cm^2/Vs) was formed ~120 nm below the wafer's surface.

Niobium (Nb) superconducting contacts were made by standard photolithography technique. First, we created a 120–140 nm deep trench by wet etching and then a ~130 nm of Nb was deposited by DC magnetron sputtering in an Ar plasma. The 130 nm thickness of Nb is about three times larger than the London penetration depth of 40 nm.

The junction has a width w = 4 μm and a length L = 850 nm in the shortest path between the two Nb electrodes (see inset in Fig. 1). The ohmic contacts were made of AuGeNi and placed 100 μm away from the junctions to prevent the influence of the normal electrons on Nb-quantum well interfaces. The quantum transport measurements were performed using a standard lock-in technique by superimposing a small *ac* signal at a frequency f = 70 Hz, and amplitude of 5 μV to the junction *dc* bias voltage and the measurements were taken in a dilution fridge at T = 50 mK and up to 800 mK.

3. Results

The false color Scanning Electron Micrograph (SEM) image of the planar Nb-$In_{0.75}Ga_{0.25}As$-Nb Josephson junction is shown in the inset of Fig. 1. The device is in the ballistic regime as the distance between two Nb electrodes L = 850 nm is an order of magnitude shorter than the corresponding elastic mean free path of $\ell_e = e^{-1}\hbar\mu_e\sqrt{2\pi n_s} \approx 2$ μm [11].

The temperature dependence of the induced superconductivity is shown in Fig. 1 where the differential resistance (dV/dI) versus bias voltage (V_{SD}) graphs at temperatures between 50 and 800 mK are plotted. A pronounced supercurrent of up to 0.2 μA was observed at zero magnetic field B and at temperature T = 50 mK. Because of the electron- and hole-like quasiparticles correlations (Andreev reflections) below the junction's T_c and for voltage biases within the superconducting gap, the induced gap and subharmonic energy gap structures (SGS) are observed.

The ratio of L/ξ_N, where ξ_N is the Bardeen-Cooper-Schrieffer (BCS) coherence length [13–15] have influence on the shape of the gap and SGS. The SGS consists of a set of pronounced conductance maxima at $V = 2\Delta/ne$ where the Δ is Nb superconducting gap, and n is an integer number. In the case of the present junction, the proximity effect induces a minigap into the 2DEG with $\Delta_{ind} = 1.76\ k_BT_c \approx 100$ μeV. This suggests that our junction with a length L = 850 nm and $\xi_N = \hbar v_{FN}/\pi\Delta_{ind}$ = 2 μm is in the short channel regime ($L/\xi_N \ll 1$). For this junction, the dimensionless interface barrier strength $Z < 0.2$ and therefore an average transmissivity $T = 1/(1 + Z^2) > 0.96$ were estimated [11]. The flat dV/dI (V_{SD}) observed within the superconducting gap is consistent with BTK model [13] (see Ref. [11] for more details).

The magnetic field dependence of the induced superconductivity is shown in Fig. 2 where the plot of dV/dI as a function of applied voltage V_{SD} at B = 1 mT is shown in the inset. Here, the SGS corresponding to $2\Delta/3e$ (blue), $2\Delta/4e$ (green), and $2\Delta/6e$ (red) are shown by arrows. We could not observe the SGS corresponding to $2\Delta/5e$. This may be due to the geometry of our junction (see the inset of Fig. 1). Here, the 2DEG and Nb both extend beyond the narrow area $L \times w$ where induced superconductivity is expected. Dephasing from the 2DEG regions either side of the junction (which are in normal state) may influence the SGS. The corresponding voltage points of the observed SGS are plotted as a function of B in Fig. 2. It is found that the SGS are strongly B dependent, with the position of the peaks bending toward zero voltage as B is increased and being totally washed out at 0.2 T.

The dI/dV versus B shows a maximum at zero B which decreases by increasing B up to 0.25 T (see Fig. 3). Above this point it reaches a constant value indicating that the junction turns into the normal state. When decreasing B to below ±0.25 T, vortex pinning in the Nb electrodes causes a hysteresis in dI/dV (B) plot. The dI/dV curve in Fig. 3 shows a symmetric shift of conductance close to zero B field for both positive and negative fields.

Here, the applied B field and the vortex penetrating the electrodes are parallel. However, when the sign of the applied B field

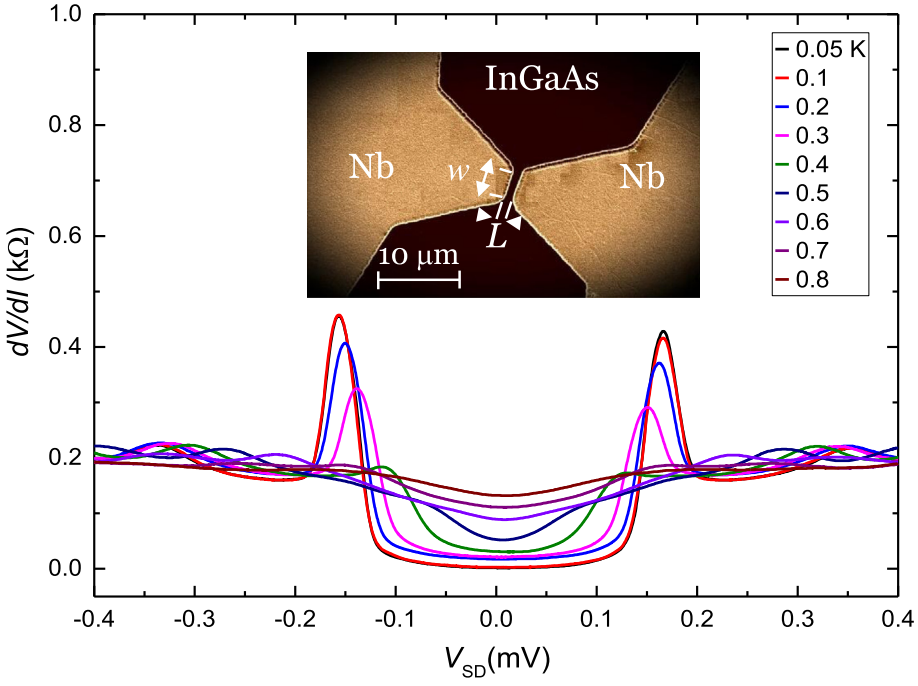

Fig. 1. The superconductor-semiconductor-superconductor Josephson junction: The differential resistance (dV/dI) versus bias voltage V_{SD} at temperatures between 50 and 800 mK. Inset: the false color scanning electron micrograph (SEM) image showing a top view of a symmetric Nb-$In_{0.75}Ga_{0.25}As$-Nb Josephson junction. The superconducting contacts are Niobium (Nb) as shown in dark-gold color in the figure. The gap size between two Nb electrodes has a length L = 850 nm and a width w = 4 μm at the shortest path. (For interpretation of the references to color in this figure legend, the reader is referred to the web version of this article.)

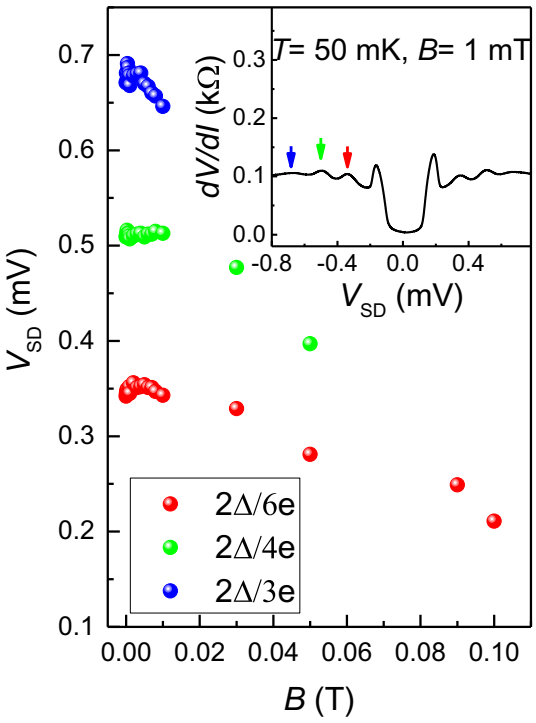

Fig. 2. Magnetic field dependence of the induced superconductivity in a ballistic Josephson junction: The blue, green and red circles (see their corresponding arrows in inset) indicate the magnetic field evolution of the induced- and subharmonic-gap structures. Inset is the dV/dI (V) measured at $B = 1$ mT and $T = 50$ mK. Arrows correspond to SGS: $2\Delta/3e$ (blue), $2\Delta/4e$ (green), and $2\Delta/6e$ (red). (For interpretation of the references to color in this figure legend, the reader is referred to the web version of this article.)

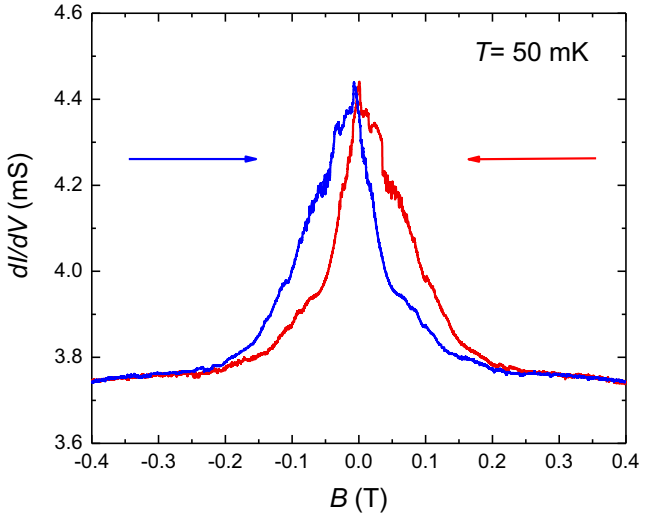

Fig. 3. Magnetoconductance oscillations and hysteresis on the differential conductance of the Nb-$In_{0.75}Ga_{0.25}As$-Nb Josephson junction: Differential conductance (dI/dV) vs. applied magnetic field B perpendicular to the junction's plane at temperature 50 mK. Arrows indicate the B sweep directions.

changes (e.g. $B < 0$ to $B > 0$), B and the pinned vortex becomes anti-parallel [16,17]. The pinned vortex may cause a phase change at the interface, and causes the appearance of the dI/dV oscillations and zero B shift.

Such oscillations have also been observed in different systems such as granular Sn wires [18], superconducting Pb nanobridges [19], and gold nanowires [20].

4. Conclusion

We have experimentally studied the proximity induced superconductivity in a hybrid Nb-$In_{0.75}Ga_{0.25}As$-Nb ballistic Josephson junction. We demonstrated the formation of highly transparent interfaces between Nb and $In_{0.75}Ga_{0.25}As$ quantum wells. The temperature and magnetic field dependences of the induced superconducting gap and subharmonic gap structures were discussed. The presented platform may be helpful for the development of integrated quantum circuitry.

Acknowledgment

Authors acknowledge financial support from EPSRC grant numbers EP/M009505/1 and EP/J017671/1. K. Delfanazari is grateful to Dr. H. Asai for helpful discussions. The data presented in this paper can be accessed at https://doi.org/10.17863/CAM.13774.

References

[1] A.F. Andreev, Thermal conductivity of the intermediate state of superconductors, Sov. Phys. JETP 19 (1964) 1228.
[2] Z. Wan et al., Induced superconductivity in high-mobility two-dimensional electron gas in gallium arsenide heterostructures, Nat. Commun. 6 (2015) 7426, https://doi.org/10.1038/ncomms8426.
[3] M. Kjaergaard et al., Quantized conductance doubling and hard gap in a two-dimensional semiconductor–superconductor heterostructure, Nat. Commun. 7 (2016) 12841, https://doi.org/10.1038/ncomms12841.
[4] T. Sand-Jespersen, J. Paaske, B.M. Andersen, K. Grove-Rasmussen, H.I. Jørgensen, M. Aagesen, C.B. Sørensen, P.E. Lindelof, K. Flensberg, J. Nygard, Kondo-enhanced Andreev tunneling in InAs nanowire quantum dots, Phys. Rev. Lett. 99 (2007) 126603.
[5] J.A.V. Dam, Y.V. Nazarov, E.P.A.M. Bakkers, S.D. Franceschi, L.P. Kouwenhoven, Supercurrent reversal in quantum dots, Nature 442 (2006) 667–670.
[6] F. Giazotto, P. Spathis, S. Roddaro, S. Biswas, F. Taddei, M. Governale, L. Sorba, A Josephson quantum electron pump, Nat. Phys. 7 (2011) 857–861.
[7] V. Mourik et al., Signatures of Majorana fermions in hybrid superconductor-semiconductor nanowire devices, Science 336 (2012) 1003–1007.
[8] L.P. Rokhinson, X. Liu, J.K. Furdyna, The fractional a.c. Josephson effect in a semiconductor-superconductor nanowire as a signature of Majorana particles, Nat. Phys. 8 (2012) 795–799.
[9] M.T. Deng et al., Majorana bound state in a coupled quantum-dot hybrid-nanowire system, Science 354 (2016) 1557–1562.
[10] A.Yu. Kitaev, Fault-tolerant quantum computation by anyons, Ann Phys 303 (2003) 2–30.
[11] K. Delfanazari, R.K. Puddy, P. Ma, T. Yi, M. Cao, Y. Gul, I. Farrer, D.A. Ritchie, H.J. Joyce, M.J. Kelly, C.G. Mith, On chip Andreev devices: hard gap and quantum transport in ballistic Nb-$In_{0.75}Ga_{0.25}As$ quantum well-Nb Josephson junctions, Adv. Mater. 29 (2017) 1701836.
[12] C. Chen, I. Farrer, S.N. Holmes, F. Sfigakis, M.P. Fletcher, H.E. Beere, D.A. Ritchie, Growth variations and scattering mechanisms in metamorphic $In_{0.75}Ga_{0.25}As$/$In_{0.75}Al_{0.25}As$ quantum wells grown by molecular beam epitaxy, J. Cryst. Growth 425 (2015) 70–75.
[13] G.E. Blonder, M. Tinkham, T.M. Klapwijk, Transition from metallic to tunneling regimes in superconducting microconstrictions: excess current, charge imbalance, and supercurrent conversion, Phys. Rev. B 25 (1982) 4515.
[14] K. Flensberg, J.B. Hansen, M. Octavio, Subharmonic energy-gap structure in superconducting weak links, Phys. Rev. B 38 (1988) 8707.
[15] H.Y. Günel, N. Borgwardt, I.E. Batov, H. Hardtdegen, K. Sladek, G. Panaitov, D. Grützmacher, Th. Schäpers, Crossover from Josephson effect to single interface Andreev reflection in asymmetric superconductor/nanowire junctions, Nano Lett. 14 (9) (2014) 4977–4981.
[16] Y. Takagaki, Transport properties of semiconductor-superconductor junctions in quantizing magnetic fields, Phy. Rev. B 57 (1998) 4009.
[17] Y. Asano, Magnetoconductance oscillations in ballistic semiconductor-superconductor junctions, Phys. Rev. B 61 (2000) 1732.
[18] A.V. Herzog, P. Xiong, R.C. Dynes, Magnetoresistance oscillations in granular Sn wires near the superconductor-insulator transition, Phys. Rev. B 58 (1998) 21.
[19] Jian Wang et al., Semiconductor-superconductor transition and magnetoresistance terraces in an ultrathin superconducting Pb nanobridge, J. Vac. Sci. Technol. B 28 (2010), https://doi.org/10.1116/1.3437016.
[20] J. Wang, C. Shi, M. Tian, Q. Zhang, N. Kumar, J. Jain, T. Mallouk, M.H.W. Chan, Proximity-induced superconductivity in nanowires: minigap state and differential magnetoresistance oscillations, Phys. Rev. Lett. 102 (2009) 247003.